

Electronic Supplementary Information

Synergistic Effect Incorporating Intra- and Inter-Molecular Charge Transfer in Nonfullerene Acceptor Molecules for High-Efficient Organic Solar Cells

Yiwen Ji,^a Lingxia Xu,^a Hang Yin,^a Bin Cui,^a Longlong Zhang,^b Xiaotao Hao^a and Kun Gao^{*a}

^a School of Physics, State Key Laboratory of Crystal Materials, Shandong University, Jinan 250100, China

^b College of Physics and Optoelectronics, Taiyuan University of Technology, Taiyuan 030024, China

* E-mail: gk@sdu.edu.cn

Iteratively solving the static equations: Considering the electronic eigenstate of a molecule $|\phi_{\mu,s}\rangle$, we can expand it on the Wannier basis, that is, $|\phi_{\mu,s}\rangle = \sum_n Z_{\mu,n,s} |n\rangle$. As such, the electronic eigenstates are obtained by solving the eigenequation of the electronic Hamiltonian, written as:

$$\begin{aligned}
& \left[U \left(\rho_{n,n,s} - \frac{1}{2} \right) + V_{\parallel} \sum_n (\rho_{n+1,n+1} + \rho_{n-1,n-1} - 2) \right] Z_{\mu,n,s} \\
& + \left[t_3 Z_{\mu,n-3,s} + \Delta_{\text{on}} Z_{\mu,n,s} \right] \left[\delta \left(\frac{n-10}{4}, \text{int} \right) + \delta \left(\frac{n-12}{4}, \text{int} \right) \right] \\
& + \left[t_3 Z_{\mu,n+3,s} + \Delta_{\text{on}} Z_{\mu,n,s} \right] \left[\delta \left(\frac{n-7}{4}, \text{int} \right) + \delta \left(\frac{n-9}{4}, \text{int} \right) \right] \\
& - \Delta'_{\text{on}} Z_{\mu,n',s} - t_{n-1,n} Z_{\mu,n-1,s} - t_{n,n+1} Z_{\mu,n+1,s} = \varepsilon_{\mu} Z_{\mu,n,s}
\end{aligned} \tag{1}$$

$\rho_{n,n,s} = \sum_{\mu} Z_{\mu,n,s}^* f_{\mu} Z_{\mu,n,s}$ is the density matrix, where f_{μ} (0 or 1) denotes the electron occupation function of electronic eigenstate $|\phi_{\mu,s}\rangle$. $\delta(i, \text{int})=1$, if $i=\text{int}$; and $\delta(i, \text{int})=0$, if $i \neq \text{int}$, where “int” means a positive integer.

On the other hand, by minimizing the total energy of the molecule, we can obtain the lattice balance equation:

$$u_{n+1} - u_n = \frac{2\alpha}{K} \left(\frac{1}{N-1} \sum_{n,s} \rho_{n,n+1,s} - \sum_s \rho_{n,n+1,s} \right) \tag{2}$$

where the fixed boundary is employed. N is the total site number of the molecule.

PDOS calculation: We separately calculate the PDOS of the central D group and terminal A groups of the molecule by:¹

$$\text{PDOS}^{\text{D(A)}}(E) = \sum_{\mu,n,s} Z_{\mu,n,s}^* Z_{\mu,n,s} \delta(E - \varepsilon_{\mu}) \tag{3}$$

$\sum_{\mu,n,s}$ means the summation for the sites of central D group or terminal A groups, ε_{μ} the eigenenergy of the electronic eigenstate $|\phi_{\mu,s}\rangle$.

Binding energy calculation for an IEx or IIEx state:

$$\begin{aligned}
E = & \sum_{\mu}^{\text{occ}} \varepsilon_{\mu} + \frac{1}{2} \sum_{j,n} K (u_{j,n+1} - u_{j,n})^2 \\
& - U \sum_{j,n} (\rho_{j,n,n,\uparrow} - \frac{1}{2})(\rho_{j,n,n,\downarrow} - \frac{1}{2}) - V_{\parallel} \sum_{j,n} (\rho_{j,n,n} - 1)(\rho_{j,n+1,n+1} - 1) \\
& - V_{\perp} \sum_{n'} (\rho_{1,n',n'} - 1)(\rho_{2,n',n'} - 1) - V_{\perp} \sum_{n'} (\rho_{1,n',n'} - 1)(\rho_{3,n',n'} - 1)
\end{aligned} \tag{4}$$

$$\Delta E_{\text{IEx(IIEx)}} = E_{\text{IEx(IIEx)}} - E_{\text{Gr}} \tag{5}$$

$$\Delta E_{\text{p}^{\pm}} = E_{\text{p}^{\pm}} - E_{\text{Gr}} \tag{6}$$

$$E_{\text{B}}^{\text{IEx}} = (\Delta E_{\text{p}^+} + \Delta E_{\text{p}^-}) - \Delta E_{\text{IEx}} \tag{7}$$

$$E_{\text{B}}^{\text{IIEx}} = (\Delta E_{\text{p}^+} + \Delta E_{\text{p}^-}) - \Delta E_{\text{IIEx}} \tag{8}$$

Equation (4) shows the total energy of the system, by which we can separately obtain the system energy lying in different states, including the ground state energy E_{Gr} , the IEx state energy E_{IEx} , the IIEx state energy E_{IIEx} , the positive polaron state energy E_{p^+} , and the negative polaron state energy E_{p^-} . “occ” indicates the sum only for the occupied electronic states, j is the molecular index. Furthermore, we can separately obtain the creation energy of an IEx state (ΔE_{IEx}), IIEx state (ΔE_{IIEx}), a positive polaron state (ΔE_{p^+}), and a negative polaron state (ΔE_{p^-}) by Equations (5) and (6). Finally, the binding energy of an IEx state ($E_{\text{B}}^{\text{IEx}}$) in a molecule and the binding energy of an IIEx state ($E_{\text{B}}^{\text{IIEx}}$) in different molecular aggregates is obtained by Equations (7) and (8), respectively.

Dissociation Efficiency Calculation of an IEx or IIEx State: The dissociation efficiency η_{IEx} (η_{IIEx}) of an IEx (IIEx) state at different temperatures (T) is estimated by employing the approximate formula introduced by Rubel et al.:²

$$\eta_{\text{IEx(IIEx)}} \approx \left[1 + (\nu_0 \tau_0)^{-1} \exp\left(\frac{E_{\text{B}}^{\text{IEx(IIEx)}}}{k_{\text{B}} T}\right) \right]^{-1} \quad (9)$$

ν_0 represents the attempt-to-escape frequency, τ_0 the average lifetime of an IEx or IIEx state, k_{B} the Boltzmann constant. According to refs. 2 and 3, we set $\nu_0=10^{13} \text{ s}^{-1}$ and $\tau_0=1 \text{ ps}$.

Parameter Details: In all simulations, unless otherwise specified, the values of model parameters are set as $t_0=2.5 \text{ eV}$, $\alpha=41.0 \text{ eV/nm}$, $K=2100 \text{ eV/nm}$, $t_1=t_2=0.05 \text{ eV}$, $t_3=0.1 \text{ eV}$, and $U=1.5 \text{ eV}$. The intra-molecular offsite Coulomb interaction strength V_{\parallel} and the inter-molecular vertical-neighbor sites Coulomb interaction strength V_{\perp} are treated as Ohno potentials $V_{\parallel(\perp)} = U / \sqrt{1 + \kappa(r_{\parallel(\perp)} / r_0)^2}$ with $\kappa=2$, $r_{\parallel}=r_0$, and $r_{\perp}=3\text{\AA}$ (κ is the screening factor, $r_0=1.22\text{\AA}$ the average nearest-neighbor lattice constant, and r_{\perp} the inter-molecular distance between vertical-neighbor sites). The inter-molecular electron hopping integral between vertical-neighbor sites is described as $t_{\perp} = \frac{t_0}{10} \exp(1 - \frac{r_{\perp}}{5})$.

Here, let's briefly explain how the values of the key parameters for the modeled NFA molecule are selected. Firstly, the key parameters determining the molecular electronic and lattice structures are the nearest-neighbor electron hopping integral for a uniform lattice structure t_0 , the electron-lattice ($e-l$) interaction constant α , the elastic constant between the nearest-neighbor sites K , and the average nearest-neighbor lattice constant r_0 . For the values of these four parameters, we refer to those chosen for a polyacetylene molecule.⁴ In

order to reflect the unique molecular geometry of the modeled NFA molecule, we further introduce t_1 , t_2 and t_3 .

Especially, to highlight the A-D-A electronic structure of the modeled NFA molecule, we employ the on-site energy difference ($\Delta_{\text{on}} + \Delta'_{\text{on}}$) between the central D group and the terminal A groups to describe its electron push-pull ability. Herein, a value range of $0 \leq (\Delta_{\text{on}} + \Delta'_{\text{on}}) \leq 0.6 \text{ eV}$ is considered to discuss the effect of the electron push-pull ability on the molecular electronic structure. Recently, we note a work by Perdigón Toro et al.,⁵ in which they calculated the intra-molecular electrostatic bias potential of the typical NFA molecule (Y6) and obtained that the value can reach up to 1.1 eV. In view of this, the value range of $0 \leq (\Delta_{\text{on}} + \Delta'_{\text{on}}) \leq 0.6 \text{ eV}$ does not overestimate the contribution of the electron push-pull ability of an actual NFA molecule.

Using these parameters, we first compare the energy gap of the modeled NFA molecule with that of some typical NFA molecules (obtained to be 1.4-1.6 eV in other works).⁶⁻⁸ As presented in Fig. 2, we can see that the HOMO/LUMO levels can be separately designed by modulating the electron-push ability (Δ_{on}) of central D group and the electron-pull ability (Δ'_{on}) of terminal A groups. Thus, the energy gap of the modeled NFA molecule can be effectively modulated by tuning the value of Δ_{on} or Δ'_{on} . For instance, we get an energy gap of 1.6 eV when we choose the value of Δ_{on} to be 0.6 eV. These findings are consistent with the experimental observations, which confirms the validity of our model description for an A-D-A type NFA molecule.

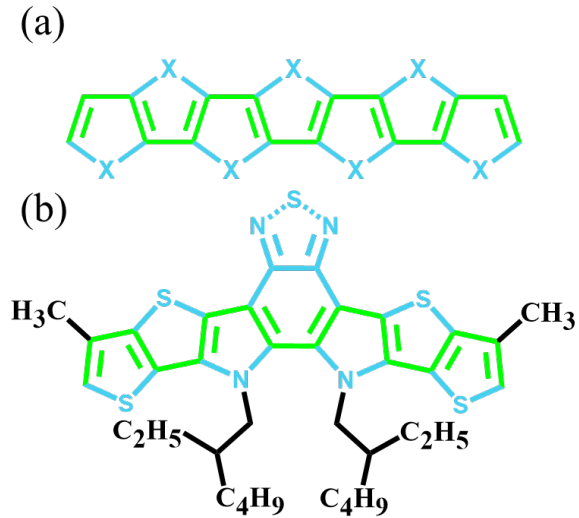


Fig. S1. The central D group structures of our modeled NFA molecule (a) and a simplified Y6 molecule (b), where the green describes the conjugated skeleton including 16 sites.

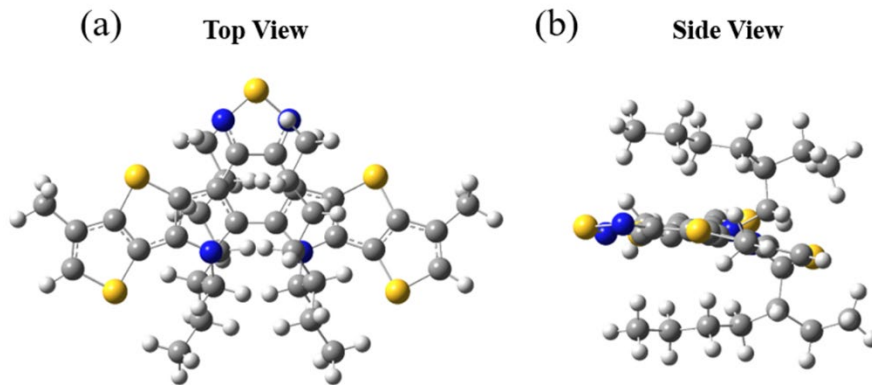


Fig. S2. Optimized molecular geometries for the central D group of the simplified Y6 molecule from top view (a) and side view (b), respectively.

In addition, we compare the lattice structure (i.e., the bond length variation $\delta r_n = u_{n+1} - u_n$) of the central D group in our modeled NFA molecule with that in a simplified Y6 molecule (see Fig. S1), where a density functional theory (DFT) calculation

at the ω B97X-D/6-31+G (d, p) level has been carried out (Gaussian 16 program package).⁹

¹⁰ In the Gaussian calculation, the 2-ethylhexyl side chains on the two nitrogen atoms of the central D group in Y6 are included, while the alkyl side chains on the thiophene units is replaced by $-\text{CH}_3$ groups for simplicity. Fig. S2 demonstrates the optimized molecular geometries for the central D group of the simplified Y6 molecule from top view (a) and side view (b), respectively. As such, distribution of the bond length variation along the central D group is presented in Fig. S3, where the model and Gaussian calculations are compared. We can see that the lattice structure obtained by our model calculation is basically consistent with that obtained by the Gaussian calculation. It further confirms the validity of our model description.

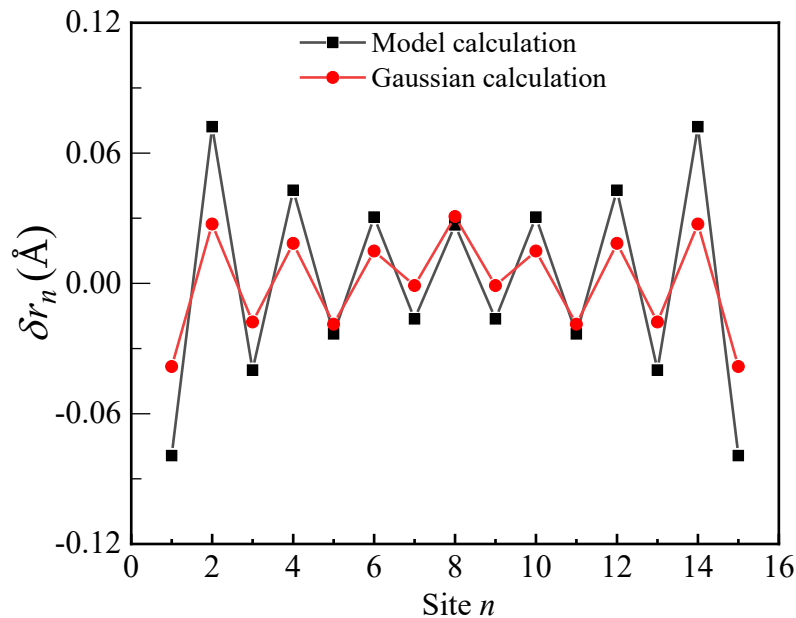


Fig. S3. Distribution of the bond length variation (i.e. $\delta r_n = u_{n+1} - u_n$) along the central D group, where the model and Gaussian calculations are compared.

Impact of the inter-molecular aggregation degree on the Inter-CT character: From Fig. S4, we can clearly see that the inter-molecular transferred charge quantity in A-to-A type J-aggregation presents an apparent reduction tendency with the increase of the value of r_{\perp} (r_{\perp} shows the inter-molecular distance, reflecting the inter-molecular aggregation degree). Thus, we can improve the Inter-CT intensity in NFA molecular aggregates by strengthening the inter-molecular aggregation degree.

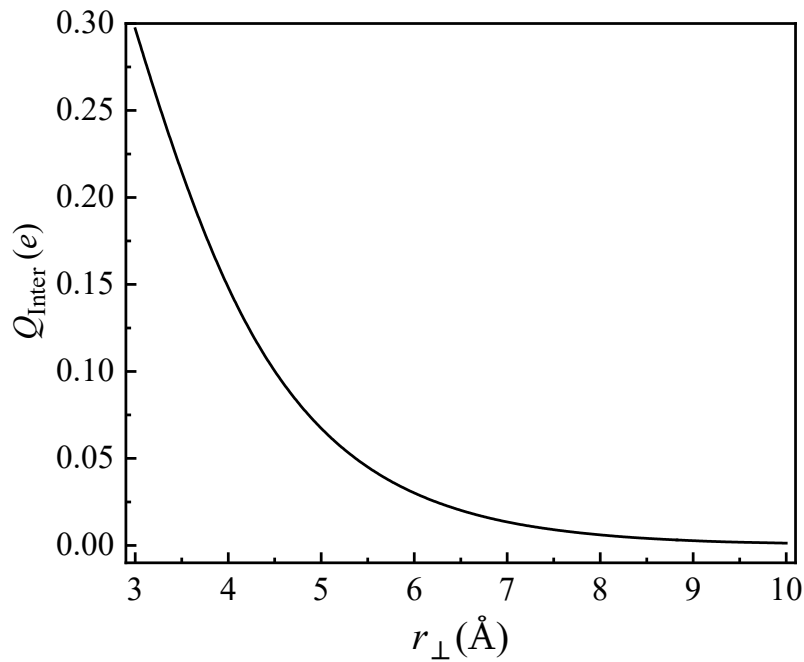


Fig. S4. The inter-molecular transferred charge quantity Q_{inter} in A-to-A type J-aggregation as a function of the inter-molecular distance r_{\perp} , where the value of Δ_{on} is fixed to be 0.6 eV

References

- 1 L. Zhang, Y. Hao, K. Gao, *Appl. Phys. Lett.*, 2020, **117**, 123301.
- 2 O. Rubel, S. D. Baranovskii, W. Stolz, F. Gebhard, *Phys. Rev. Lett.*, 2008, **100**, 196602.
- 3 A. V. Nenashev, S. D. Baranovskii, M. Wiemer, F. Jansson, R. Österbacka, A. V. Dvurechenskii, F. Gebhard, *Phys. Rev. B.*, 2011, **84**, 035210.
- 4 W. P. Su, J. R. Schrieffer, A. J. Heeger, *Phys. Rev. Lett.*, 1979, **42**, 1698-1701.
- 5 L. Perdigón-Toro, H. Zhang, A. Markina, J. Yuan, S. M. Hosseini, C. M. Wolff, G. Zou, M. Stolterfoht, Y. Zou, F. Gao, D. Andrienko, S. Shoaee, D. Neher, *Adv. Mater.*, 2020, **32**, 1906763.
- 6 D. Qian, Z. Zheng, H. Yao, W. Tress, T. R. Hopper, S. Chen, S. Li, J. Liu, S. Chen, J. Zhang, X. K. Liu, B. Gao, L. Ouyang, Y. Jin, G. Pozina, I. A. Buyanova, W. M. Chen, O. Inganäs, V. Coropceanu, J. L. Bredas, H. Yan, J. Hou, F. Zhang, A. Bakulin, F. Gao, *Nat. Mater.*, 2017, **17**, 703-709.
- 7 Y. Lin, Z. G. Zhang, H. Bai, J. Wang, Y. Yao, Y. Li, D. Zhu, X. Zhan, *Energy Environ. Sci.*, 2015, **8**, 610.
- 8 G. Zhang, J. Zhao, P. C. Y. Chow, K. Jiang, J. Zhang, Z. Zhu, J. Zhang, F. Huang, H. Yan, *Chem. Rev.*, 2018, **118**, 3447–3507.
- 9 J.-D. Chai, M. Head-Gordon, *Phys. Chem. Chem. Phys.*, 2008, **10**, 6615-6620.
- 10 M. J. Frisch, G. W. Trucks, H. B. Schlegel, G. E. Scuseria, M. A. Robb, J. R. Cheeseman, G. Scalmani, V. Barone, G. A. Petersson, H. Nakatsuji, X. Li, M. Caricato, A. V. Marenich, J. Bloino, B. G. Janesko, R. Gomperts, B. Mennucci, H. P. Hratchian,

J. V. Ortiz, A. F. Izmaylov, J. L. Sonnenberg, D. Williams-Young, F. Ding, F. Lipparini, F. Egidi, J. Goings, B. Peng, A. Petrone, T. Henderson, D. Ranasinghe, V. G. Zakrzewski, J. Gao, N. Rega, G. Zheng, W. Liang, M. Hada, M. Ehara, K. Toyota, R. Fukuda, J. Hasegawa, M. Ishida, T. Nakajima, Y. Honda, O. Kitao, H. Nakai, T. Vreven, K. Throssell, J. A. Montgomery, J. Jr., E. Peralta, F. Ogliaro, M. J. Bearpark, J. J. Heyd, E. N. Brothers, K. N. Kudin, V. N. Staroverov, T. A. Keith, R. Kobayashi, J. Normand, K. Raghavachari, A. P. Rendell, J. C. Burant, S. S. Iyengar, J. Tomasi, M. Cossi, J. M. Millam, M. Klene, C. Adamo, R. Cammi, J. W. Ochterski, R. L. Martin, K. Morokuma, O. Farkas, J. B. Foresman and D. J. Fox, Gaussian 16, Gaussian, Inc.: Wallingford, CT, 2016.